

Excited-state-donor-to-acceptor transitions in the photoluminescence spectrum of GaAs and InP

B. J. Skromme and G. E. Stillman

*Electrical Engineering Research Laboratory, Materials Research Laboratory and Coordinated Science Laboratory,
University of Illinois at Urbana-Champaign, Urbana, Illinois 61801*

(Received 16 September 1983; revised manuscript received 31 October 1983)

In addition to the normally observed conduction-band-to-acceptor and ground-state-donor-to-acceptor transition peaks in the low-temperature photoluminescence spectrum of high-purity GaAs and InP, we report for the first time the observation of an additional peak in the spectrum, which we attribute to transitions from donors in their first excited state to neutral acceptors. This peak appears between the normally observed conduction-band-to-acceptor ($e-A^0$) and ground-state-donor-to-acceptor ($D_{n=1}^0-A^0$) peaks. The theory of Kamiya and Wagner is generalized to include this process and predicts line shapes in excellent agreement with experiment.

INTRODUCTION

It is well known that for each different shallow acceptor species in a high-purity GaAs or InP sample, two distinct broad peaks are observed in the low-temperature photoluminescence (PL) spectrum.¹ There is general agreement that the lower-energy peak in both GaAs (Ref. 2) and InP (Ref. 3) is due to distant ground-state ($n=1$) donor-acceptor pair recombination, which we denote ($D_{n=1}^0-A^0$), but the mechanism responsible for the higher-energy peak has been the subject of some dispute. While this peak was originally ascribed to excited-state-donor-to-acceptor recombination, denoted ($D_{n=2}^0-A^0$), in GaAs,⁴ later magneto-optical⁵⁻⁸ and time-resolved measurements⁹ clearly ruled out this interpretation in favor of the conduction-band-to-acceptor ($e-A^0$) model, which has been almost universally adopted.

Some dispute persists as to the origin of the similarly behaving high-energy peak in InP. Recent arguments have been presented, similar to the earlier discussion of GaAs,⁴ favoring the ($D_{n=2}^0-A^0$) interpretation in InP.¹⁰ In this paper, we show the arguments used in assigning the high-energy peaks in Refs. 4 and 10 to the ($D_{n=2}^0-A^0$) mechanism to be invalid, and we present data which for the first time permits observation of a third small peak between the two previously observed peaks corresponding to each of three different acceptors in GaAs and one acceptor in InP. This third peak is assigned here to the ($D_{n=2}^0-A^0$) process, while the two previously observed peaks are attributed to the ($e-A^0$) and ($D_{n=1}^0-A^0$) mechanisms. A theoretical calculation of the overall line shape, including the ($D_{n=2}^0-A^0$) mechanism, is presented and is shown to give excellent agreement with experiment. In addition, we consider several alternative models and show that they do not give a satisfactory explanation of the data. We conclude with a comparison of this recombination process to analogous mechanisms that have been reported in other semiconductors.

EXPERIMENTAL

The samples that were used in this study consisted of high-purity n -type GaAs samples grown by AsCl_3 and

AsH_3 -VPE (vapor-phase epitaxy), liquid-phase epitaxy (LPE), metal organic chemical vapor deposition (MOCVD), and molecular-beam epitaxy (MBE) in over 35 different laboratories, along with n -type InP samples grown by PH_3 -VPE, LPE, and bulk-growth methods in several laboratories. The ($D_{n=2}^0-A^0$) peak was resolved in 40 of the approximately 165 GaAs samples that were measured, and in two of about 65 InP samples. Some of the reasons that this peak was frequently undetectable will be discussed below. The average 77-K mobility of the GaAs samples is about $101\,000\text{ cm}^2/\text{V s}$, and the average 77-K carrier concentration is about $1.5 \times 10^{14}\text{ cm}^{-3}$. Hall data are listed in Table I for the samples whose spectra will be shown here. Luminescence measurements were performed with the sample freely suspended in either liquid He for measurements at 4.2 or 1.7 K and in flowing gaseous He for measurements above 4.2 K. The unfocused beam of an Ar^+ laser operating at 5145 \AA was used as the excitation source, with a power level of 5 mW or less for the spectra shown here. Sample heating by the laser beam is therefore expected to be negligible. The luminescence was dispersed by an $f/9$, 1.0-m spectrometer and detected with a cooled S-1 or GaAs photomultiplier tube using dc detection. Typical spectral resolution was around 0.2 \AA for most of the spectra shown here.

RESULTS

A series of PL spectra at several different temperatures are shown in Fig. 1 for a MOCVD GaAs sample. The principal ($D_{n=1}^0-A^0$) and ($e-A^0$) peaks which are observed in this sample are those due to the acceptor C, although a trace of another ($D_{n=1}^0-A^0$) peak due to Zn at 1.4861 eV is also evident at low temperature. Increases in the temperature result in thermal ionization of the shallow donor levels into the conduction band, causing the observed decline in the intensity of the ($D_{n=1}^0-A^0$) recombination peak with a concomitant increase in the intensity of the ($e-A^0$) peak. The feature which is of primary interest here is the additional peak on the low-energy side of the ($e-A^0$) peak in the spectra taken at the lowest temperatures. As the temperature increases, this peak is reduced to a shoulder on the ($e-A^0$) peak, and is finally masked completely by the

TABLE I. 300- and 77-K electrical characteristics of the samples whose spectra are shown in the following.

Sample	Material	Growth technique	$n_{300\text{ K}}$ (cm^{-3})	$n_{77\text{ K}}$ (cm^{-3})	$\mu_{300\text{ K}}$ ($\text{cm}^2/\text{V s}$)	$\mu_{77\text{ K}}$ ($\text{cm}^2/\text{V s}$)
Toshiba 004	GaAs	MOCVD	9.2×10^{13}	8.0×10^{13}	7700	97 000
Bell J10120	GaAs	MBE	1.5×10^{14}	1.4×10^{14}	6240	115 000
Fujitsu 3761	GaAs	AsCl ₃ -VPE	9.9×10^{13}	1.1×10^{14}	6460	92 900
Cornell SM-30	GaAs	LPE	1.5×10^{14}	1.8×10^{14}	7960	117 000
Forschungsinstitut P406	InP	LPE	3.7×10^{14}	6.3×10^{14}	5100	74 900

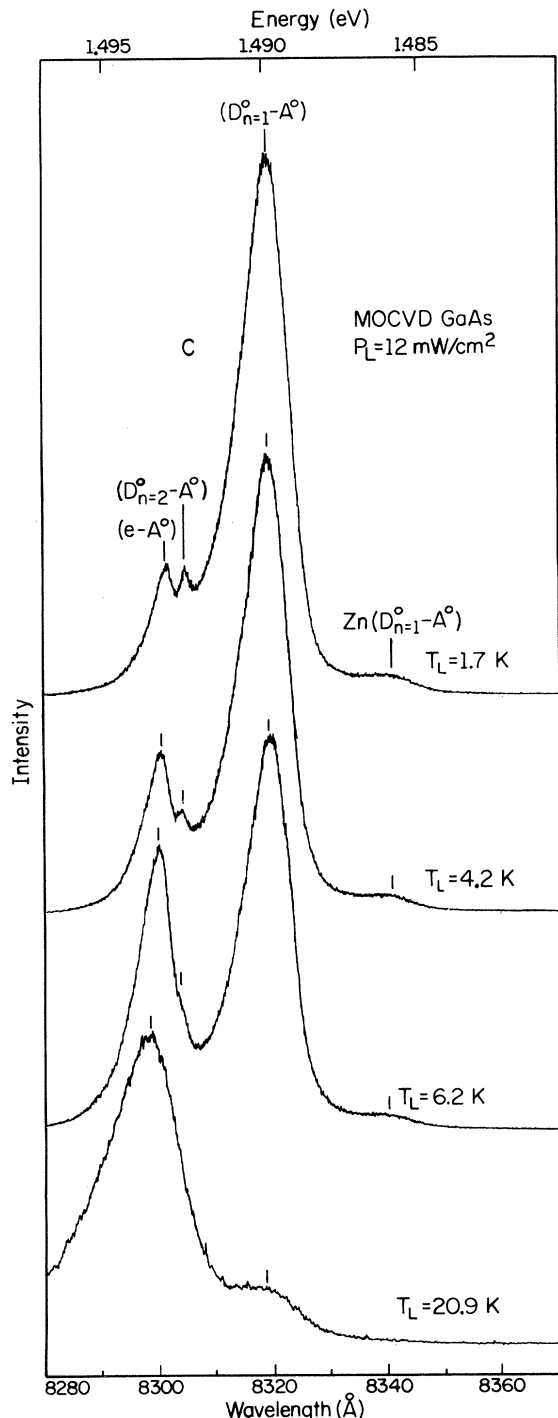


FIG. 1. PL spectrum of an MOCVD GaAs sample (Toshiba 004) at four different lattice temperatures.

growing ($e-A^0$) peak at the higher temperatures.

The additional peak has not been previously reported in GaAs or InP, although the ($e-A^0$) and ($D_{n=1}^0-A^0$) peaks are well known; we assign it here to the ($D_{n=2}^0-A^0$) process discussed above. The ($e-A^0$), ($D_{n=2}^0-A^0$), and ($D_{n=1}^0-A^0$) peaks for C acceptors in the sample of Fig. 1 occur at 1.493 12, 1.492 54, and 1.489 85 eV, respectively (these are the positions at 1.7 K). It should be noted that our identification of the ($D_{n=2}^0-A^0$) peak is at variance with previous reports, which attributed the peak that we label ($e-A^0$) to the ($D_{n=2}^0-A^0$) mechanism in GaAs (Ref. 4) and InP.¹⁰ Reasons why these previous assignments should be regarded as incorrect will be discussed in a later section.

We have found that the ($D_{n=2}^0-A^0$) peak can be observed most often for C acceptors in GaAs, for reasons to be discussed later, but we were also able to discern a similar peak for Si acceptors in three LPE samples and for Zn acceptors in thirteen AsCl₃-VPE samples. In Fig. 2 we show low-temperature (1.7-K) spectra for three different samples. The bottom curve shows the spectrum of an MBE GaAs sample which contains only C acceptors and the usual "defect"-related luminescence at lower energies (not shown). A distinct peak due to the ($D_{n=2}^0-A^0$) mechanism is also observed. The middle curve is for an AsCl₃-VPE sample containing almost entirely Zn acceptors with only a minute trace of C. The ($D_{n=2}^0-A^0$) peak for Zn acceptors is visible on the low-energy side of the ($e-A^0$) peak. While the ($D_{n=1}^0-A^0$) peak for C occurs at almost exactly the same location as the Zn ($e-A^0$) and ($D_{n=2}^0-A^0$) peaks, a comparison of the intensities of the ($e-A^0$) peaks due to Zn and C at higher temperatures indicated that the C acceptors would make a negligible contribution to the spectrum in the vicinity of the Zn peaks, and thus cannot account for the additional peak. The top spectrum is for an LPE sample dominated by Si acceptors and again shows a small ($D_{n=2}^0-A^0$) peak; the peaks to higher energy are due to Mg and C acceptors. In all cases above, the ($D_{n=2}^0-A^0$) peaks were found to be repeatably present.

A very similar type of peak was observed in the PL spectrum of an LPE InP sample containing one residual acceptor, as shown in Fig. 3 for four different temperatures. The residual acceptor in this sample was first reported by Hess *et al.*, who denoted it " A_1 ",¹¹ we have recently identified the chemical origin of this peak as either Mg or Be.¹² The temperature dependence of the ($D_{n=2}^0-A^0$) peak in this spectrum follows very closely that which is observed for GaAs in Fig. 1. In this spectrum, the ($e-A^0$), ($D_{n=2}^0-A^0$), and ($D_{n=1}^0-A^0$) peaks occur at 1.382 84, 1.381 99, and 1.378 58 eV, respectively.

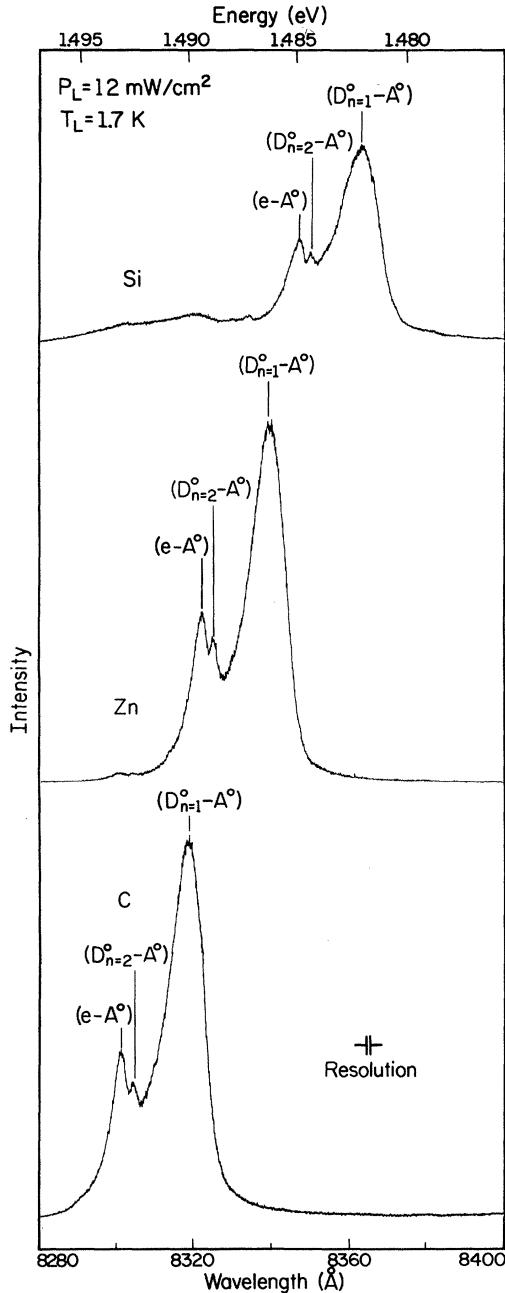


FIG. 2. PL spectra of an MBE GaAs sample containing C acceptors (Bell J10120), an AsCl₃-VPE sample containing Zn acceptors (Fujitsu 3761), and an LPE sample containing Si acceptors (Cornell SM-30), all at $T_L = 1.7$ K.

THEORETICAL LINE-SHAPE CALCULATION

It is qualitatively clear that the $(D_{n=2}^0-A^0)$ recombination mechanism should produce a peak just slightly below the $(e-A^0)$ peak in energy, yet well above the $(D_{n=1}^0-A^0)$ transition for the acceptor in question. In order to quantitatively predict the relative spacings and the temperature dependences of these three peaks, however, it is necessary to perform a detailed calculation. The energy of the pho-

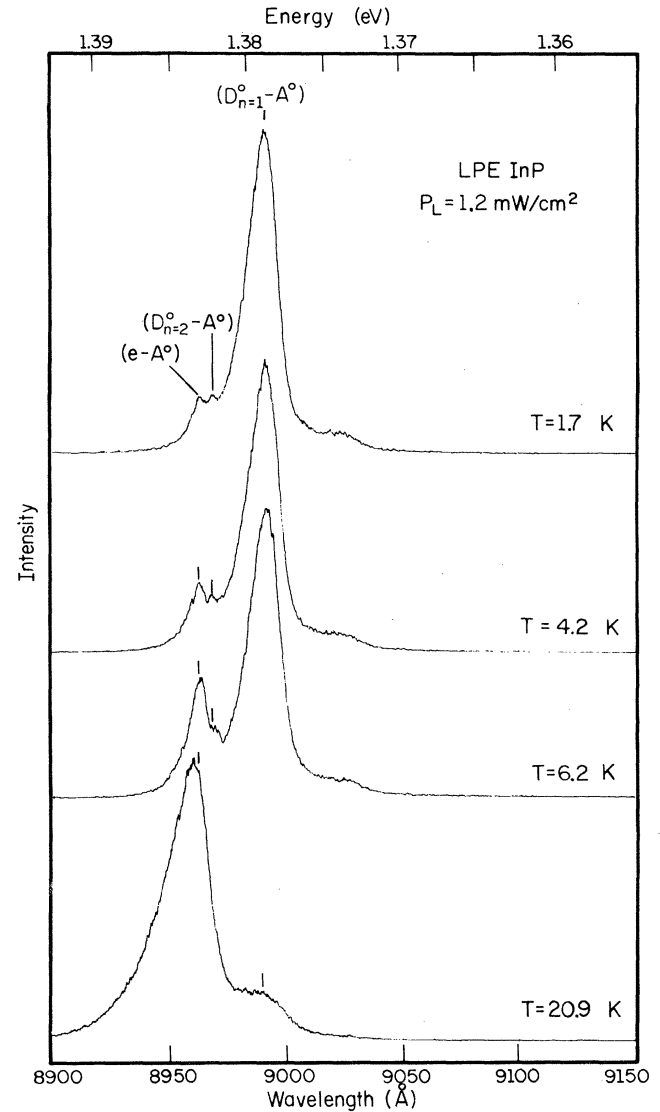


FIG. 3. PL spectrum of an LPE InP sample (Forschungsinstitut P406) at four different lattice temperatures.

ton produced by $(D_{n=1}^0-A^0)$ recombination involving a reasonably distant $n=1$ donor-acceptor pair which is separated by a distance R_1 is given by the well-known expression

$$E_1(R_1) = \hbar\omega = E_g - E_A - E_D + \frac{e^2}{4\pi\epsilon_0\epsilon_r R_1}, \quad (1)$$

where E_1 is the photon energy, E_g is the band gap, E_A and E_D are the ionization energies of the acceptor and donor, respectively, and ϵ_r is the low-frequency relative dielectric constant of the material. The position of the peak of the $(D_{n=1}^0-A^0)$ band, in the absence of competing recombination processes, is therefore determined by the assumed random distribution of neutral acceptors and donors in their ground states, which can be characterized by an average-pair-separation distance. The average pair separation determines the magnitude of the Coulomb shift of the peak. The $(D_{n=2}^0-A^0)$ peak will also be subject to a

Coulomb shift, but the average pair separation in this case will be substantially larger due to the smaller number of donors which are in their first excited state. The Coulomb shift of the $(D_{n=2}^0-A^0)$ peak will therefore be much smaller than the shift of the $(D_{n=1}^0-A^0)$ peak. The position and breadth of the $(e-A^0)$ band depends on the thermal distribution of electrons in the conduction band and can be determined by the theory of Eagles.¹³

A complication arises in calculating the overall line shape in the presence of several competing recombination mechanisms involving the photoneutralized acceptors. Processes which compete with $(D_{n=1}^0-A^0)$ recombination, such as $(e-A^0)$, $(D_{n=2}^0-A^0)$, or nonradiative recombination involving acceptors, will have a stronger influence on the recombination of relatively distant $(D_{n=1}^0-A^0)$ pairs, whose lifetime is fairly long, as compared to relatively close $(D_{n=1}^0-A^0)$ pairs whose radiative lifetime is much shorter.^{2,14} Since the more distant pairs correspond to lower-energy photons, according to Eq. (1), the net effect of the competing processes is to shift the peak of the $(D_{n=1}^0-A^0)$ band to higher energies. Similar remarks apply to the $(D_{n=2}^0-A^0)$ peak, although here the shift will be less due to the greater spatial extent of the $n=2$ donor wave functions and correspondingly much shorter lifetimes.

The above effects were first quantified for the case of competing $(e-A^0)$ and $(D_{n=1}^0-A^0)$ recombination in GaAs by Kamiya and Wagner.¹⁵ In the following, we generalize their theory to include four additional competing recombination processes, which involve $(D_{n=2}^0-A^0)$ pairs with the donor in one of its four degenerate $n=2$ states. It will be shown quantitatively that due to the effects discussed above, the separation of the $(D_{n=1}^0-A^0)$ and $(D_{n=2}^0-A^0)$ peaks is less than $3E_D/4$.

The first problem in extending the theory of Ref. 15 (hereafter denoted KW for Kamiya-Wagner theory) is to calculate the transition rate for $(D_{n=2}^0-A^0)$ recombination, involving a donor in one of its four degenerate $n=2$ states. The transition rates will be denoted, e.g., $W_{1s,2p^0}$, where the first subscript applies to the acceptor wave function and the second to the donor. An expression for $W_{1s,1s}(R_1)$ is given as Eq. (7) of KW; the analogous ex-

pression for, e.g., $W_{1s,2p^0}(R_{2p^0})$, where R_{2p^0} is the distance between a neutral acceptor and its nearest-neighbor neutral donor in its $2p^0$ state, is given by the following:

$$W_{1s,2p^0}(R_{2p^0}) = \frac{4e^2 n' E_2}{4\pi\epsilon_0 m^2 \hbar^2 c^3} |M_{cv}|^2 I_{1s,2p^0}^2. \quad (2)$$

Here, e and m are the electronic charge and mass, c is the speed of light in vacuum, n' is the refractive index, ϵ_0 is free-space permittivity, \hbar is Planck's constant divided by 2π , and M_{cv} is the matrix element between the conduction- and valence-band states. The quantity $I_{1s,2p^0}$ is the overlap integral of the hydrogenic $2p^0$ donor wave function with the $1s$ wave function of the acceptor (assumed to be hydrogenic) which is located a distance R_{2p^0} from the donor. The formulas applicable to the other $n=2$ states of the donor may be obtained from Eq. (2) with an appropriate change of subscripts; one must also substitute E_1 [as given by Eq. (1)] for E_2 in obtaining the formula for $n=1$ donors. In this latter case the formula for $I_{1s,1s}$ is given by Eq. (8) of KW. The energy of the emitted photon for $(D_{n=2}^0-A^0)$ recombination is denoted E_2 , which is independent of which particular degenerate $n=2$ donor state is involved, and is given by the expression

$$E_2(R_2) = E_g - E_A - \frac{E_D}{4} + \frac{e^2}{4\pi\epsilon_0\epsilon_r R_2}. \quad (3)$$

One may evaluate the various overlap integrals analytically for the $n=2$ donor states with the same technique originally used by Zeiger for $I_{1s,1s}$,¹⁶ namely, the problem is transformed into the prolate spheroidal coordinates μ , ν , and ψ , where

$$\mu = (r + |\vec{r} - \vec{R}|)/R, \quad \nu = (r - |\vec{r} - \vec{R}|)/R,$$

and

$$\psi = \tan^{-1}(y/x).$$

We assume that donor is at the origin and the acceptor is at $(0,0,R)$. The use of this transformation for this type of problem is discussed by Baym.¹⁷ One obtains

$$I_{1s,2s} = \frac{8\alpha'^{3/2}}{\rho(\alpha'^2-1)^4} \{ e^{-\rho} [2\alpha'\rho(1-\alpha'^4) + 8\alpha'(2\alpha'^2+1)] + e^{-\alpha'\rho} [\rho(1+6\alpha'^2-7\alpha'^4) - 8\alpha'(2\alpha'^2+1) - \alpha'\rho^2(\alpha'^2-1)^2] \}, \quad (5)$$

$$I_{1s,2p^0} = \frac{64\alpha'^{3/2}}{\rho^2(\alpha'^2-1)^4} \left[e^{-\rho} \left[\frac{\alpha'^2\rho^2(\alpha'^2-1)}{2} - 3\alpha'^2(\rho+1) \right] + e^{-\alpha'\rho} \left[\frac{\alpha'\rho^3(\alpha'^2-1)^2}{8} + \alpha'^2\rho^2(\alpha'^2-1) + 3\alpha'^2(\alpha'\rho+1) \right] \right], \quad (6)$$

$$|I_{1s,2p^\pm}| = \frac{3\pi\rho\alpha'^{5/2}}{\sqrt{2}(\alpha'^2-1)^3} \left[\mp(\alpha'-1)(\alpha'^2-1)K_0 \left[\frac{\rho}{2}(\alpha'+1) \right] I_1 \left[\mp\frac{\rho}{2}(\alpha'-1) \right] \right. \\ \left. + (\alpha'+1)(\alpha'^2-1)K_1 \left[\frac{\rho}{2}(\alpha'+1) \right] I_0 \left[\mp\frac{\rho}{2}(\alpha'-1) \right] \right. \\ \left. \pm \frac{16\alpha'}{\rho} K_1 \left[\frac{\rho}{2}(\alpha'+1) \right] I_1 \left[\mp\frac{\rho}{2}(\alpha'-1) \right] \right]. \quad (7)$$

In writing these equations we have adopted a dimensionless notation similar to that of Zeiger,¹⁶ namely

$$\alpha = \frac{a_A}{2a_D},$$

$$\rho = \frac{R}{a_A},$$

and

$$a_{A,D} = \frac{e^2}{8\pi\epsilon_r\epsilon_0 E_{A,D}}. \quad (8)$$

In Eq. (7) the upper and lower sets of signs are to be taken in the cases where $\alpha' < 1$ or $\alpha' > 1$, respectively (the former case applies for GaAs or InP). The notations I_0 , K_0 , I_1 , and K_1 denote modified Bessel functions of the first and second kinds, of orders 0 and 1, respectively.

A plot of the contributions of the various transition rates for each of the cases $1s-2s$, $1s-2p^0$, and $1s-2p^\pm$, which were computed above is given in Fig. 4(a) together with the total recombination rates involving $n=1$ and 2 donors. The various scales on the abscissa correspond to the pair separations of the $(D_{n=1}^0-A^0)$ and $(D_{n=2}^0-A^0)$ pairs, and the wavelengths of the emitted photons correspond to those values of pair separation. The transition rates for donors in the various $n=2$ degenerate states may be compared directly and summed because the statistical distribution of pair-separation distances is the same for pairs involving each of the degenerate states, as will be shown below. It is apparent that the contribution of the $1s-2p^\pm$ pairs is essentially negligible and may be dropped, simplifying the computation. In Fig. 4(b) the transition rates are plotted as a function of pair-separation distance. The structure in $W_{1s,2s}$ at small separations is due to the node in the donor $2s$ wave function at $r=2a_D$ crossing the acceptor wave function. The expressions for the rates, however, are only strictly valid for reasonably large separation such that the respective wave functions are not appreciably perturbed; Eqs. (1) and (3) also apply only to this case. It is seen that the transition rate for $(D_{n=2}^0-A^0)$ pairs is much higher than for $(D_{n=1}^0-A^0)$ pairs of comparable separation, as was asserted earlier.

An expression for the $(e-A^0)$ transition rate, according to the theory of Eagles,¹³ is obtained by combining Eqs. (1)–(3) of KW,¹⁸

$$W_{e,A}(E) = \left[\frac{32\sqrt{2}a_A^3 m_c^{*3/2}}{\pi\hbar^3} \right] \left[\frac{4e^2 n' |M_{cv}|^2}{4\pi\epsilon_0 m^2 \hbar^2 c^3} \right] E(E - E_g + E_A)^{1/2} \exp\left[-\frac{E - E_g + E_A - E_F}{kT_e} \right], \quad (9)$$

where T_e is the electron temperature, E is the photon energy, and E_F is the Fermi level. The total recombination rate $W_{e,A}^{\text{tot}}$ is then obtained by integrating Eq. (9),

$$W_{e,A}^{\text{tot}} = \frac{1}{2} C_0 \sqrt{\pi} (kT_e)^{3/2} \exp(E_F/kT_e) \left(\frac{3}{2} kT_e + E_g - E_A \right), \quad (10)$$

where C_0 is the product of the first two terms in large parentheses in Eq. (9).

We now need to calculate the Fermi level as a function of N_D , N_A , and T_e , allowing for the influence of the discrete excited states of the donor. We use an equation analogous to Eq. (4) of KW,¹⁸ generalized according to the discussion in Blakemore,¹⁹

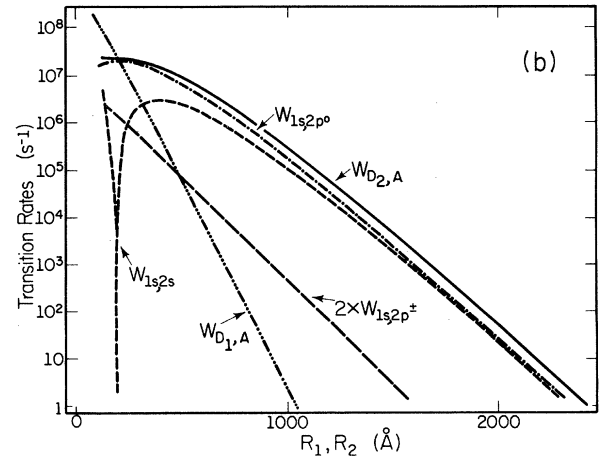
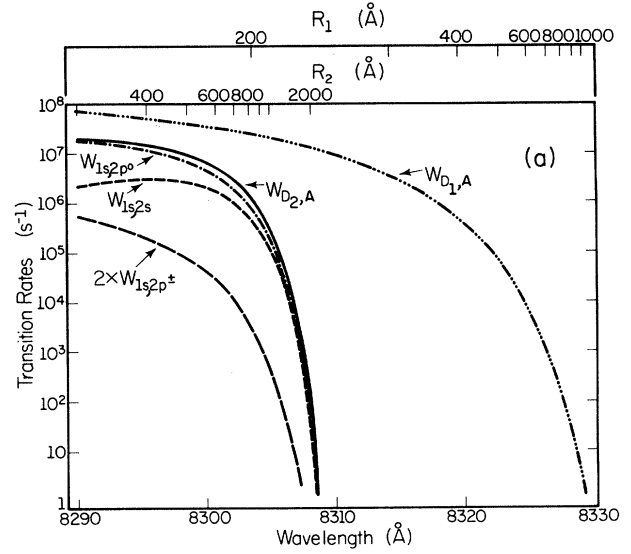


FIG. 4. (a) Transition rates for $(D_{n=1}^0-A^0)$ recombination (denoted $W_{D_{1,A}}$), components of $(D_{n=2}^0-A^0)$ recombination involving donors in their $2s$, $2p^0$, and $2p^\pm$ states (denoted $W_{1s,2s}$, $W_{1s,2p^0}$, and $W_{1s,2p^\pm}$, respectively), and the total $(D_{n=2}^0-A^0)$ recombination rate (denoted $W_{D_{2,A}}$). The abscissas correspond to the wavelengths of the emitted photons in each case, as well as the corresponding pair separations for $(D_{n=1}^0-A^0)$ and $(D_{n=2}^0-A^0)$ pairs (R_1 and R_2 , respectively). (b) The same transition rates plotted as a function of pair separation.

$$E_F = kT_e \ln \left[\frac{2(N_D - N_A)}{(N_c + N_A S) + [(N_c + N_A S)^2 + 4N_c(N_D - N_A)S]^{1/2}} \right], \quad (11)$$

with

$$S \equiv \sum_{r=1}^{r_{\max}} 2r^2 \exp \left[\frac{E_D/r^2 - \Delta E}{kT_e} \right], \quad (12)$$

and N_c is given by Eq. (5) of KW. In this equation, we have allowed for the reduction in the effective thermal ionization energy of the donors, due to the banding of the higher excited states of the donors which then merge with the conduction band.²⁰ This reduction in energy is denoted ΔE ; it is a function of the doping as illustrated graphically in Ref. 20. The value of ΔE determines the number of discrete excited states to be included in the sum in Eq. (12); i.e. r_{\max} is determined by ΔE . No allowance for ΔE was made in the original work by KW, which probably accounts for the excessively low compensation ratios they obtained. Inclusion of this effect was found to be very important in obtaining good agreement between optically and electrically derived values of the compensation ratio in a recent study of VPE InP.²¹

Given the position of the Fermi level from Eq. (11), the total concentrations of neutral donors in their ground state, n_1 and in their first excited states n_2 are

$$n_1 = \frac{2N_D \exp \left[\frac{E_F + E_D - \Delta E}{kT_e} \right]}{1 + \exp \left[\frac{E_F}{kT_e} \right] S} \quad (13)$$

and

$$n_2 = \frac{8N_D \exp \left[\frac{E_F + E_D/4 - \Delta E}{kT_e} \right]}{1 + \exp \left[\frac{E_F}{kT_e} \right] S}, \quad (14)$$

where S is still given by Eq. (12). The concentration of neutral donors in any of the particular $n=2$ states is the same,

$$n_{2s} = n_{2p^0} = n_{2p^+} = n_{2p^-} = n_2/4. \quad (15)$$

Assuming a random (noncorrelated) distribution of neutral donors and acceptors in the lattice, in an n -type sample, the probability of a neutral acceptor having a nearest-neighbor neutral donor in its i th state a distance R_i away is

$$P_D^i(R) = 4\pi n_i R_i^2 \exp\left(-\frac{4}{3}\pi R_i^3 n_i\right), \quad i = 1s, 2s, 2p^0, 2p^+, 2p^- \quad (16)$$

in analogy to Eq. (9) of KW.¹⁸ Note that KW used N_D as the neutral donor concentration but this neglects the effects of compensation as well as the thermal depopulation of the donors at higher temperatures. If the pumping rate were indeed sufficiently high to photoneutralize all of the shallow donors, as assumed in effect by KW, then unperturbed thermal-equilibrium statistics would no longer apply and the whole theory breaks down. It is also not sufficient to multiply Eq. (16) by the probability that a donor is neutral, as done in Ref. 21, since this factor must also be included in the exponent to keep the probability distribution function normalized.

We are now ready to calculate the stationary neutral acceptor concentration n_A^0 for weak-pumping conditions, following KW. We have

$$\frac{n_A^0}{N_A W_{h,A}} = \int_0^\infty \int_0^\infty \int_0^\infty \int_0^\infty \int_0^\infty P_D^{1s}(R_1) P_D^{2s}(R_{2s}) P_D^{2p^0}(R_{2p^0}) P_D^{2p^+}(R_{2p^+}) P_D^{2p^-}(R_{2p^-}) \\ \times \frac{P_A^0(R_1, R_{2s}, R_{2p^0}, R_{2p^+}, R_{2p^-}) dR_1 dR_{2s} dR_{2p^0} dR_{2p^+} dR_{2p^-}}{W_{h,A}}, \quad (17)$$

with

$$\frac{P_A^0(R_1, R_{2s}, R_{2p^0}, R_{2p^+}, R_{2p^-})}{W_{h,A}} \\ \approx \frac{1}{W_{e,A}^{\text{tot}} + W_{1s,1s}(R_1) + W_{1s,2s}(R_{2s}) + W_{1s,2p^0}(R_{2p^0}) + W_{1s,2p^+}(R_{2p^+}) + W_{1s,2p^-}(R_{2p^-}) + W_{\text{nr}}}. \quad (18)$$

Here, $W_{h,A}$ is the hole-capture rate for ionized acceptors, W_{nr} is the nonradiative recombination rate of neutral acceptors, and $P_A^0(R_1, R_{2s}, R_{2p^0}, R_{2p^+}, R_{2p^-})$ denotes the probability of being neutral for an acceptor whose nearest-neighbor neutral $n=1$ donor is a distance R_1 away and whose nearest-neighbor $2s$, $2p^0$, $2p^+$, and $2p^-$ donors are located a dis-

tance R_{2s} , R_{2p^0} , R_{2p^+} , and R_{2p^-} away, respectively. The other quantities in these equations are given by Eqs. (2), (10), and (16). The quantity n_A^0 is normalized to the unknown value of $W_{h,A}$ to facilitate comparisons of relative peak heights below.

The expression for n_A^0 in Eq. (17) can be evaluated numerically to a reasonably good approximation by neglecting the transition rates for the $n=2$ donors in the denominator of the integrand in Eq. (18). It is then necessary to integrate over only one dimension. The accuracy of this approximation may be checked by expanding Eq. (18) using the binomial series between appropriate finite limits of integration and then combining the truncation error due to the finite limits with the error resulting from truncation of the series.

Having computed n_A^0 , we may immediately write down expressions for the normalized line shapes of the three recombination processes, $(e-A^0)$, $(D_{n=2}^0-A^0)$, and $(D_{n=1}^0-A^0)$, in order to compare the relative magnitudes of the three peaks as a function of temperature and doping. In analogy with KW, we have

$$\frac{I_{e,A}(E)}{N_A W_{h,A}} = W_{e,A}(E) \frac{n_A^0}{N_A W_{h,A}}, \quad (19)$$

$$\begin{aligned} \frac{I_{D_{2,A}}(E)}{N_A W_{h,A}} = P_D^{2s}(R_2(E)) \left| \frac{dR_2(E)}{dE} \right| & \left[W_{1s,2s}(R_2(E)) P_A^0(\infty, R_2(E), \infty, \infty, \infty) \right. \\ & \left. + W_{1s,2p^0}(R_2(E)) P_A^0(\infty, \infty, R_2(E), \infty, \infty) + 2W_{1s,2p^\pm}(R_2(E)) P_A^0(\infty, \infty, \infty, R_2(E), \infty) \right], \end{aligned} \quad (20)$$

and

$$\frac{I_{D_{1,A}}(E)}{N_A W_{h,A}} = P_D^{1s}(R_1(E)) \left| \frac{dR_1(E)}{dE} \right| W_{1s,1s}(R_1(E)) P_A^0(R_1(E), \infty, \infty, \infty, \infty). \quad (21)$$

Here, $I_{D_{2,A}}$ denotes the total intensity of the recombination radiation from $(D_{n=2}^0-A^0)$ pairs, which is the sum of terms representing the radiation resulting from each of the degenerate $n=2$ donor states. The intensity of $(D_{n=1}^0-A^0)$ recombination is denoted $I_{D_{1,A}}$ and $I_{e,A}$ is the intensity of $(e-A^0)$ recombination radiation. In Eq. (20) we used $P_D^{2s}(R_2)$ as the common multiplicative factor since the Poisson distributions for all of the degenerate $n=2$ states are identical in light of Eq. (15). The use of ∞ as one of the distances which are the arguments of P_A^0 is tantamount to neglecting the corresponding recombination rate in the expression for P_A^0 in Eq. (18), since all the recombination rates vanish for infinitely large separation distances. Strictly speaking, one should include these recombination rates and integrate each term in Eq. (20) over the four distance variables which we have set to ∞ , multiplying by the four appropriate Poisson distributions in each case. The approximation we have used in writing Eq. (20) is equivalent to the approximation discussed above to be used in evaluating n_A^0 from Eq. (17).

We have calculated the overall luminescent line shape for the GaAs sample of Fig. 1 using Eqs. (19)–(21). A fit to the carrier concentration as a function of temperature, measured by Hall effect, was used to obtain values of N_D , N_A , and ΔE , assuming one discrete excited state. The value of $E_g(T_L=0)$ was adjusted to fit the position of the $(e-A^0)$ peak at 1.7 K, while the temperature variation of the band gap was taken to be $\Delta E_g = -3.8 \times 10^{-4} T_L^2$ meV, based on temperature-dependent PL measurements of the position of the neutral-donor bound-exciton peak from 1.7–21 K. The value of W_{nr} was chosen to give the correct spacing between the $(D_{n=1}^0-A^0)$ and $(e-A^0)$ peaks

at $T_L = 1.7$ K. The values of electron temperature T_e corresponding to each value of lattice temperature T_L were determined by a fit to the experimental data. The electron temperature was found to be significantly higher than the lattice temperature due to the photoexcitation for low values of T_L , in agreement with previous findings.⁷ At higher T_L , electron-phonon scattering becomes more frequent and T_e approaches T_L . The results of the calculation are shown in Fig. 5.

A comparison of Figs. 1 and 5 shows that the peak positions and qualitative temperature dependence of the experimental data are in excellent accord with the predictions of our model. The calculated position of the $(D_{n=2}^0-A^0)$ peak is 1.492 68 eV as opposed to the measured value of 1.492 54 eV. The separation of the $(D_{n=1}^0-A^0)$ pairs is 420 Å at the peak of their recombination curve while the separation of the $(D_{n=2}^0-A^0)$ pairs at the peak of their curve is 959 Å. The shift in the $(D_{n=2}^0-A^0)$ peak as a result of the competing recombination paths was found to be only 1.13 meV as compared to a shift of 1.79 meV in the $(D_{n=1}^0-A^0)$ peak, for the reasons discussed earlier. The above remarks all apply to the $T_L = 1.7$ K, $T_e = 7.2$ K curves. While the experimentally observed $(D_{n=1}^0-A^0)$ peak in Fig. 1 at 20.9 K appears to be larger than that which is theoretically predicted, this effect is due in part to the contribution of the Zn $(e-A^0)$ peak which is coincident with it. The relative magnitudes of the $(D_{n=1}^0-A^0)$ peaks due to Zn and C at 1.7 K might suggest that this contribution would be insignificant, but differential thermal ionization of the shallower acceptor C strongly favors the Zn $(e-A^0)$ peak over that of C at this temperature.²²

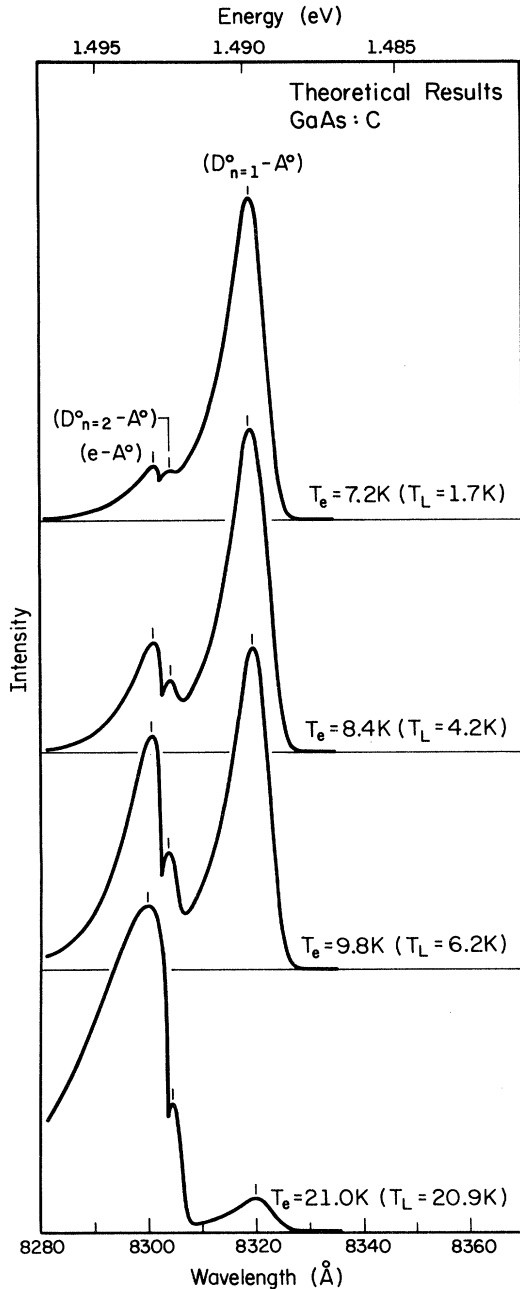


FIG. 5. Results of a theoretical calculation of the PL line shapes for the sample of Fig. 1 at four different electron temperatures (T_e). The values $N_D=4.50 \times 10^{14} \text{ cm}^{-3}$, $N_A=2.47 \times 10^{14} \text{ cm}^{-3}$, and $\Delta E=1.25 \text{ meV}$ as obtained from a fit to variable-temperature Hall-effect data were used in generating the curves (ΔE is the effective lowering of the conduction-band edge due to banding of the higher excited states of the donors). The values $E_g(T=0)=1.51914 \text{ eV}$ and nonradiative recombination rate $\mathcal{W}_{nr}=2.5 \times 10^5 \text{ s}^{-1}$ were used to fit the data of Fig. 1. All other parameter values were taken from Ref. 15.

DISCUSSION

There are several limitations to the accuracy of the above theory. Firstly, the acceptor wave functions are not

really hydrogenic as assumed, and in actuality show a strongly nonhydrogenic character due to the valence-band degeneracy.⁸ Secondly, possible correlation effects in the distribution of donors and acceptors in the crystal or in the donor occupation have been neglected. Third, the temperature dependence of the nonradiative recombination rate has been neglected. Finally, the line-shape calculation itself ignored the effects of band tailing for the conduction band due to the higher excited states of the donors, which have broadened and merged with the conduction band at these doping levels.²⁰ [We did, however, include this effect in calculating the position of the Fermi level, Eq. (11).] The low-energy side of the $(e-A^0)$ peak will therefore be broadened somewhat compared to our theoretical results, which accounts for the inability to experimentally resolve the $(D_{n=2}^0-A^0)$ peak from the $(e-A^0)$ peak at higher temperatures. We may extend these considerations to explain why the Eagles model¹³ is frequently unable to accurately fit the low-energy side of the $(e-A^0)$ peak when the $(D_{n=2}^0-A^0)$ peak is not separately resolved.^{15,23} On the other hand, in p -type material where the $(D_{n=1}^0-A^0)$ luminescence has been reported to be negligible, the Eagles model has yielded good fits to the line shape of the entire $(e-A^0)$ peak.⁷ This observation is consistent with the above model. We may conclude that the excess broadening of the $(e-A^0)$ peak can be accounted for by the excited states of the donor without invoking phonon-coupled processes as has previously been done.¹⁵

The Eagles model for the $(e-A^0)$ line shape predicts that the peak of this emission will shift to higher energies with increasing temperature by an amount $\frac{1}{2}kT_e$. Experimentally, we always observe such a shift for both GaAs and InP; for example, in the sample of Fig. 1 the $(e-A^0)$ peak shifts from 1.49312 eV at $T_L=1.7 \text{ K}$ to 1.49366 eV at $T_L=20.9 \text{ K}$. The increase in energy due to the $\frac{1}{2}kT_e$ term over this range ($T_e=7.2\text{--}21.0 \text{ K}$) is +0.59 meV, compared to the experimental value of +0.54 meV. However, the reduction in E_g due to the increase in lattice temperature should also be taken into account, which from our measurements (see above) is -0.17 meV over this range. The resulting net theoretical shift is thus +0.42 meV, which compares reasonably well with the experimental value of +0.54 meV.

It should be noted that expressions which have been given elsewhere for the variation of E_g as a function of T_L for GaAs and InP strongly overestimate the shrinkage of the band gap (ΔE_g) over the range 0–20 K. The expressions given by Ashen *et al.*,²² Varshni,²⁴ Panish and Casey,²⁵ and Thurmond,²⁶ give $\Delta E_g = -0.79, -0.66, -0.80,$ and -1.06 meV , respectively, for $T_L=21 \text{ K}$. These values imply a net shift of $-0.20, -0.07, -0.21,$ and -0.47 meV , respectively, in the position of the $(e-A^0)$ peak going from 1.7 to 21 K, in contrast to the experimentally observed *positive* shift. Similarly, the expression given by Varshni²⁴ for InP implies $\Delta E_g = -0.62 \text{ meV}$, which would imply a negative net shift in the $(e-A^0)$ position also for InP. Our measurements of $\Delta E_g(T_L)$ were based on the position of the principal neutral-donor bound-exciton (D^0, X) peak from 1.7 to 21 K in both GaAs and InP. The bound-exciton system possesses no

kinetic energy and therefore follows the band gap precisely. Our data on two GaAs samples was fit well by the expression given above, $\Delta E_g = -3.8 \times 10^{-4} T_L^2$ meV, while for the two InP samples we measured, the best fit was given by $\Delta E_g = -5.8 \times 10^{-4} T_L^2$ meV. The positive energy shift of the $(e-A^0)$ peak position is in accord with the Eagles model for both GaAs and InP if the correct values for $\Delta E_g(T)$ are used.

It is rather remarkable, considering the immense volume of literature which has been published on PL measurements of high-purity GaAs and InP, that the $(D_{n=2}^0-A^0)$ peak we report has not been previously observed. In the samples we studied, the $(D_{n=2}^0-A^0)$ peak was resolved distinctly in only 40 of 165 GaAs samples, and then it was typically discernible only for a rather narrow range of excitation intensities and temperatures. For GaAs the optimum conditions were about $T_L = 1.7-4$ K and $P_L \approx 12$ mW/cm²; for InP the optimum excitation level was closer to $P_L \approx 1.2$ mW/cm². A number of reasons can be given for the difficulties encountered in resolving this peak.

It is obviously necessary that the instrumental resolution be sufficient to resolve the peak, which may be difficult to achieve at low excitation levels. We note that this peak was clearly resolved much more frequently in the GaAs samples which were measured after starting to use the GaAs photomultiplier tube, whose sensitivity allowed higher resolution than the S-1 tube did. Further, the samples must, of course, be sufficiently pure that the first excited states of the donors have not merged with the conduction band; this gives the restriction $N_D \lesssim 7 \times 10^{14}$ cm⁻³ for GaAs.²⁰ In addition, the presence of more than one acceptor level in a sample frequently results in the overlap of the $(e-A^0)$ band due to one acceptor with the $(D_{n=1}^0-A^0)$ band due to a second acceptor, e.g., C and Zn in GaAs. The $(D_{n=2}^0-A^0)$ peak of the deeper acceptor is almost certain to be obscured in this case. This explains why we observed the extra peak most frequently for C acceptors in GaAs, since it is the shallowest acceptor and its $(e-A^0)$ peak cannot be overlapped. In the AsCl₃-VPE samples where the extra peak could be resolved for Zn acceptors, C acceptors were typically absent or present only in trace amounts. A final requirement is that a significant amount of $(e-A^0)$ recombination be present at low lattice temperatures (≤ 4 K), which places a minimum value on the compensation level. Given all of the above restrictions, it is not too surprising that the $(D_{n=2}^0-A^0)$ peak is only rarely discernible.

There are several alternative models that one could propose to explain the new peak that we observe, other than the $(D_{n=2}^0-A^0)$ mechanism. It could be hypothesized that the observation of a "double" peak in the vicinity of the $(e-A^0)$ recombination peak could actually be due to some sort of self-absorption "notch" in the normal $(e-A^0)$ peak. However, the position of the $(e-A^0)$ peak that grows to prominence at the higher temperatures in Figs. 1 and 3 corresponds very closely to the position of the highest-energy peak at low temperature and not to the position of the dip between the two peaks, ruling out this interpretation.

One might also propose that the new peak is actually

the $(e-A^0)$ peak of another acceptor level with only slightly different ionization energy. However, no corresponding double $(D_{n=1}^0-A^0)$ peak is ever observed, and the relative magnitudes of the two " $(e-A^0)$ " peaks do not remain constant as a function of temperature as one would expect in this model. Further, the observation of this type of structure in the spectra corresponding to three different acceptors in GaAs and one in InP makes this interpretation seem quite improbable.

Finally, the new peak could be attributed to exciton recombination involving excitons bound either to some deep center or, perhaps, to ionized acceptors. The excitation intensity dependence of the peak is not, however, typical of exciton recombination, since the peak height does not increase strongly in magnitude at high excitation intensities. A number of deeply bound exciton lines, such as excitons bound to deep O donors,²² were observed in this part of the spectrum but their intensity always increased strongly at high excitation levels. Furthermore, the bulk of the theoretical evidence indicates that ionized-acceptor bound-exciton complexes should not be stable in GaAs or InP.²⁷ One may also easily rule out the possibility that the new peaks are just "two-hole" satellites of the neutral-acceptor bound-exciton peaks. While two-hole transitions are evident in many (though not all) of the samples in this study at high excitation intensity (e.g., 2–40 W/cm²), they are rarely if ever discernible under the low-excitation-intensity conditions (≈ 12 mW/cm²) used for the spectra shown here. High excitation levels are necessary to increase the strengths of the bound-exciton lines relative to that of the background $(e-A^0)$ and (D^0-A^0) peaks, which saturate at relatively low power levels. Moreover, the two-hole replicas, when observed, occur at precisely the energies previously reported for them,²² which are not at all coincident with the observed positions of the $(D_{n=2}^0-A^0)$ peaks in the same samples. The two-hole replicas generally display the characteristic doublet structure²² which has never been found in any of the $(D_{n=2}^0-A^0)$ peaks. Given the inadequacies of these alternative models and the agreement between our model and the experimental line shapes, we conclude that $(D_{n=2}^0-A^0)$ recombination is in fact responsible for the new peak.

One may compare the present conclusions to similar results obtained elsewhere, both in GaAs and InP and in other materials. Previous papers dealing with GaAs (Ref. 4) and InP (Ref. 10) have ascribed the peak that we label $(e-A^0)$ recombination to the $(D_{n=2}^0-A^0)$ process. However, these assignments do not appear to be correct. For GaAs, ample evidence from magneto-optical studies exists, showing that the shift of the $(e-A^0)$ peak is linear in a magnetic field, as opposed to the quadratic field dependence of the $(D_{n=1}^0-A^0)$ peaks;^{5,6} a structure in the $(e-A^0)$ peak corresponding to the Landau levels of the conduction band has also been resolved.^{7,8} These data leave little doubt as to the nature of the high-energy peak in GaAs as being $(e-A^0)$ transitions.

Magnetic field data have not yet been reported for InP, and some dispute persists as to the nature of the high-energy peak in this material.¹⁰ Given the overall similarities between the PL spectra of GaAs and InP, it would be very surprising if two totally different physical processes

were responsible for the similarly behaving peaks in the two materials. Nonetheless, it was argued in Ref. 10 that the straight-line dependence observed when plotting the logarithm of the relative intensities of the two peaks versus $1/kT$ over the temperature range 9–21 K is characteristic of the high-energy peak being due to $(D_{n=2}^0-A^0)$ and not $(e-A^0)$ recombination, particularly if the photoexcited sample is highly degenerate. We first note that the sample in Ref. 10 was not nearly so degenerate as claimed. Their calculation of the Fermi level in the presence of photoexcitation used a photon flux of $10^{24} \text{ cm}^{-3} \text{ s}^{-1}$, while the stated excitation intensity of 20 mW/cm² corresponds to a flux of only $4.5 \times 10^{20} \text{ cm}^{-2} \text{ s}^{-1}$, assuming a diffusion length of 1 μm and a reflectivity of 0.3. The use of this flux and the lifetime of 15 ns, which they assumed, yields $E_F = -5.5 \text{ meV}$, which is obviously not well into the conduction band as they found using the incorrect value of photon flux. In fact a model such as the present one, which assumes nondegenerate carrier statistics, would apply.

A nearly-straight-line dependence of the logarithm of the $I_{e,A}/I_{D_{1,A}}$ ratio versus $1/kT_e$ over the temperature range studied in Refs. 4 and 10 does in fact result from our model, even though $\ln(n/n_1)$ does not vary linearly with $1/kT_e$ over this range. This phenomenon is due to the complicated dependence of the $I_{D_{1,A}}$ intensity on n_1 through the Poisson distribution of the pair-separation distances, as illustrated by Eqs. (21) and (16). In Fig. 6 we show the theoretically calculated variation of the integrated $I_{e,A}/I_{D_{1,A}}$ intensity ratio for the sample of Figs. 1 and 5 for the range $7 \leq T_e \leq 21 \text{ K}$. It is seen that a straight line of slope 5.49 meV fits the data to a very good approximation (correlation coefficient equal to 0.999 64) over this range. At lower electron temperatures the points deviate from the straight-line approximation, but this range of electron temperatures is not experimentally accessible due to heating of the electrons by the photoexcitation.

We conclude that our identification of the high-energy peak in both GaAs and InP as $(e-A^0)$ recombination is

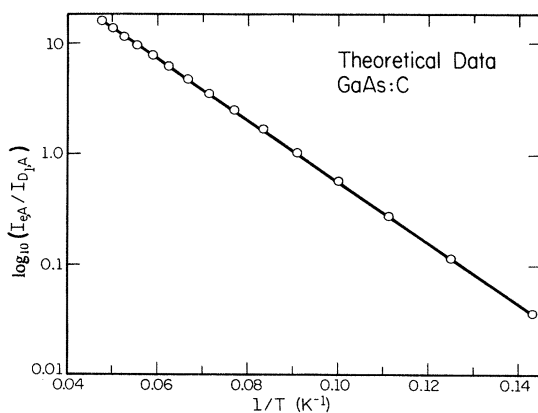


FIG. 6. Semilogarithmic plot of the theoretically calculated ratio $\log_{10}(I_{e,A}/I_{D_{1,A}})$ vs $1/T_e$ over the range $7 \leq T_e \leq 21 \text{ K}$ and a straight-line fit to the data points. The parameters used were those of Fig. 5. The slope of the line yields an activation energy of 5.49 meV.

consistent with the straight-line dependence observed over the temperature range studied in Refs. 4 and 10. Further, the clearly observable broadening of the $(e-A^0)$ peak at higher temperatures in Figs. 1 and 3, due to the broadening of the kinetic-energy distribution of the conduction-band electrons, confirms our identification. Such broadening was not observed in Refs. 4 and 10, presumably due to the initially broader peaks in the less pure samples used in those studies.

In principle, the *inverse* of the $(D_{n=2}^0-A^0)$ recombination process in GaAs and InP should be visible in excitation spectroscopy. In this technique, a tunable dye laser is used to resonantly excite donor-acceptor pairs over a narrow range of separation distances, where the donor, acceptor, or both, are in one of their *s*-like or *p*-like excited states. The experimental spectra which have been reported for InP (Refs. 28–30) and GaAs,^{31,32} however, show only evidence of acceptor excited states, and not of any excited states of the donors. The failure to observe excited donor states in these studies is most likely due to the limited purity levels of the samples which were used.

Some evidence exists for the occurrence of mechanisms analogous to $(D_{n=2}^0-A^0)$ recombination in other semiconductors. In GaP:S:C, it was suggested that pair luminescence involving excited-state C acceptors might be taking place, i.e., $(D^0-A_{n=2}^0)$ recombination;³³ however, a subsequently corrected value of the band-gap energy later led to the conclusion that this was not the case.³⁴ In CdS, Reynolds and Collins reported two series of discrete (D^0-A^0) pair lines, which were attributed to $(D^0-A_{n=1}^0)$ and $(D^0-A_{n=2}^0)$ recombination, respectively, involving the same deep (160 meV) acceptors.³⁵ To the best of our knowledge, however, the present work is the first correct identification of the $(D_{n=2}^0-A^0)$ process in any semiconductor material.

CONCLUSIONS

We have reported the observation of a new small peak on the low-energy side of the $(e-A^0)$ peaks associated with C, Zn, and Si acceptors in GaAs and with one acceptor in InP. This peak has been modeled as excited-state-donor-to-acceptor pair $(D_{n=2}^0-A^0)$ luminescence. Calculation of the transition rates for $(D_{n=2}^0-A^0)$ recombination for each of the four degenerate $n=2$ donor states was performed and these rates were incorporated into a generalized version of the theory of KW (Ref. 15) for competing $(e-A^0)$ and (D^0-A^0) recombination. The theoretical line shapes generated by this theory were shown as a function of temperature for a GaAs sample and were found to agree well with the experimental results. The quantity $\log_{10}(I_{e,A}/I_{D_{1,A}})$ calculated from the theoretical results was found to vary in an approximately linear manner as a function of $1/kT_e$ over the range $7 \leq T_e \leq 21 \text{ K}$, discounting earlier reports that such a linear relationship would not be expected if the highest-energy peak is assigned to $(e-A^0)$ recombination as we have done.^{4,10} The identification of the highest-energy peak as $(e-A^0)$ and not $(D_{n=2}^0-A^0)$ recombination, supported by the observation of the separate $(D_{n=2}^0-A^0)$ peak, supports the validity of the theory of Ref. 15 for the optical determination of compen-

sation ratios. Excess broadening of the low-energy side of the ($e-A^0$) peak has been accounted for in terms of the banded excited states of the donors.

ACKNOWLEDGMENTS

We would like to express our sincerest gratitude to the many crystal growers who supplied the samples used in this study, and in particular to T. Nakanisi and T. Udagawa of Toshiba, A. Shibatomi of Fujitsu, J. C. M. Hwang of AT&T Bell Laboratories, S. Tiwari and L. F.

Eastman of Cornell, and E. Kuphal of the Forschungsinstitut der DBP beim FTZ, whose samples were depicted above. We would also like to thank T. R. Lepkowski for the variable-temperature Hall-effect data. This work was supported by the U. S. Air Force Office of Scientific Research under Contract No. AFOSR-83-0030, the U.S. Defense Department Advanced Research Projects Agency under Contract No. N00014-83-K-0137, the U. S. Joint Services Electronics Program (U.S. Army, U. S. Navy, and U. S. Air Force) under Contract No. N00014-79-C-0424, and the National Science Foundation under Contract No. NSF-DMR-80-20250.

-
- ¹See the review by P. J. Dean, *Prog. Cryst. Growth Charact.* **5**, 89 (1982), and references therein to the original work.
- ²R. Dingle, *Phys. Rev.* **184**, 788 (1969).
- ³U. Heim, O. Röder, H. J. Queisser, and M. Pilkuhn, *J. Lumin.* **1-2**, 542 (1970).
- ⁴Jagdeep Shah, R. C. C. Leite, and J. P. Gordon, *Phys. Rev.* **176**, 938 (1968).
- ⁵J. A. Rossi, C. M. Wolfe, and J. O. Dimmock, *Phys. Rev. Lett.* **25**, 1614 (1970).
- ⁶F. Willmann, W. Dreybrodt, M. Bettini, E. Bauser, and D. Bimberg, *Phys. Status Solidi B* **60**, 751 (1973).
- ⁷W. Rühle and E. Göbel, *Phys. Status Solidi B* **78**, 311 (1976).
- ⁸D. Bimberg, *Phys. Rev. B* **18**, 1794 (1978).
- ⁹R. Ulbrich, *Phys. Rev. B* **8**, 5719 (1973).
- ¹⁰H. Burkhard, E. Kuphal, F. Kuchar, and R. Meisels, in *Gallium Arsenide and Related Compounds, Vienna, 1980*, edited by H. W. Thim (Institute of Physics, Bristol, 1981), p. 659.
- ¹¹K. Hess, N. Stath, and K. W. Benz, *J. Electrochem. Soc.* **121**, 1208 (1974).
- ¹²B. J. Skromme, G. E. Stillman, J. D. Oberstar, and S. S. Chan, *J. Electron. Mater.* (to be published).
- ¹³D. M. Eagles, *J. Phys. Chem. Solids* **16**, 76 (1960).
- ¹⁴Takeshi Kamiya and Elmar Wagner, *J. Appl. Phys.* **47**, 3219 (1976).
- ¹⁵Takeshi Kamiya and Elmar Wagner, *J. Appl. Phys.* **48**, 1928 (1977).
- ¹⁶H. J. Zeiger, *J. Appl. Phys.* **35**, 1657 (1964).
- ¹⁷Gordon Baym, *Lectures on Quantum Mechanics* (Benjamin, Reading, Mass., 1973), p. 475.
- ¹⁸Please note the following typographical errors in Ref. 9. Equation (2) is missing a factor of the photon energy E . The first N_c in Eq. (4) should be N_D and a bracket is missing. Equation (9) is missing a factor of N_D . Equation (16) should have a $-E_F$ added to the terms in the exponential. Note that our equations all use mks units while Ref. 9 used cgs units. Also, an error in their machine calculation of $n(T)$ resulted in the bottom curve of their Fig. 3 and the three curves in Fig. 6 being incorrect. Figure 4 may also have been affected but we do not know W_{nr} for those curves.
- ¹⁹J. S. Blakemore, *Semiconductor Statistics* (Pergamon, New York, 1962), p. 143.
- ²⁰G. E. Stillman and C. M. Wolfe, *Thin Solid Films* **31**, 69 (1976).
- ²¹C. Pickering, P. R. Tapster, P. J. Dean, and D. J. Ashen, in *Gallium Arsenide and Related Compounds, Albuquerque, 1982*, edited by G. E. Stillman (Institute of Physics, Bristol, 1983), p. 469.
- ²²D. J. Ashen, P. J. Dean, D. T. J. Hurle, J. B. Mullin, A. M. White, and P. D. Greene, *J. Phys. Chem. Solids* **36**, 1041 (1975).
- ²³W. Schairer and N. Stath, *J. Appl. Phys.* **43**, 447 (1972).
- ²⁴Y. P. Varshni, *Physica (Utrecht)* **34**, 149 (1967).
- ²⁵M. B. Panish and H. C. Casey, Jr., *J. Appl. Phys.* **40**, 163 (1969).
- ²⁶C. D. Thurmond, *J. Electrochem. Soc.* **122**, 1133 (1975).
- ²⁷See, P. J. Dean and D. C. Herbert, in *Excitons*, edited by K. Cho (Springer, New York, 1979), p. 55, and references therein.
- ²⁸P. J. Dean, D. J. Robbins, and S. G. Bishop, *J. Phys. C* **12**, 5567 (1979).
- ²⁹P. J. Dean, D. J. Robbins, and S. G. Bishop, *Solid State Commun.* **32**, 379 (1979).
- ³⁰D. Barthruff and H. Haspeklo, *J. Lumin.* **24-25**, 181 (1981).
- ³¹A. T. Hunter and T. C. McGill, *Appl. Phys. Lett.* **40**, 169 (1982).
- ³²D. W. Kisker, H. Tews, and W. Rehm, *J. Appl. Phys.* **54**, 1332 (1983).
- ³³P. J. Dean, in *Progress in Solid State Chemistry*, edited by J. O. McCaldin and G. Somorjai (Pergamon, Oxford, 1973), Vol. 8, p. 1.
- ³⁴P. J. Dean, *Prog. Cryst. Growth Charact.* **5**, 89 (1982).
- ³⁵D. C. Reynolds and T. C. Collins, *Phys. Rev.* **188**, 1267 (1969).